

Experimental demonstration of a programmable quantum computer by NMR

Jaehyun Kim, Jae-Seung Lee, Taesoon Hwang, and Soonchil Lee*

Department of Physics, Korea Advanced Institute of Science and Technology, Daejeon 305-701, South Korea

Received 23 June 2003; revised 25 September 2003

Abstract

A programmable quantum computer is experimentally demonstrated by nuclear magnetic resonance using one qubit for the program and two qubits for data. A non-separable two-qubit operation is performed in a programmable way to show the successful demonstration. Projective measurements required in the programmable quantum computer are simulated by averaging the results of experiments just like when producing an effective pure state.

© 2003 Elsevier Inc. All rights reserved.

Keywords: Quantum computer; Quantum information science; Qubit; Programmable; Quantum algorithm

1. Introduction

Quantum operations or quantum algorithms are implemented by the corresponding quantum circuits or quantum gate arrays, which consist of elementary gates such as CNOT gates and single-qubit rotations [1]. Usually, different quantum circuits are used depending on the computations of interest. On the other hand, a certain fixed quantum gate array can execute various quantum operations if it can handle a *program state* that contains the information about the operations to be performed. This is called a *programmable quantum gate array*. That is, a unitary operator U , which is applied to a *data state* $|d\rangle$, is encoded into the program state $|U\rangle$, and the programmable gate array G makes the whole state evolve as $G(|U\rangle \otimes |d\rangle) = |U'\rangle \otimes (U|d\rangle)$, where $|U'\rangle$ is some residual state.

Nielsen and Chuang [2] have shown that it is not possible to make a deterministic universal quantum gate array, which can carry out arbitrary quantum operations in a programmable way, because there are infinitely many different (up to overall phases) quantum operations that should be represented by the program states orthogonal to each other. However, an infinite

size of a quantum register for the orthogonal representation of all these quantum operations is not feasible. Recently, Preskill [3] and Vidal et al. [4] have suggested a programmable quantum gate array that can execute a single-qubit rotation about z -axis with an arbitrary angle. This gate array is of finite size and thus feasible. But it succeeds only probabilistically. Some of the authors and a colleague [5] have generalized this circuit to perform arbitrary operations of self-inverse generators, including single-qubit rotations about z -axis, and have suggested a scheme for a probabilistic universal gate array.

In this work, we have experimentally demonstrated a programmable quantum computer by nuclear magnetic resonance (NMR). It is not a complete implementation of the universal quantum computer because we have implemented only a single execution of our circuit while it is required to repeatedly execute the circuit to realize arbitrary operations [5]. This is mainly due to the fact that in NMR experiments it is not possible to realize a projective measurement, which is necessary in the scheme [6]. However, we have employed a method to simulate the projective measurement, originally suggested by Collins [7] for an expectation value quantum search, and successfully demonstrated the experimental feasibility of the programmable quantum computer.

* Corresponding author. Fax: +82-428692510.

E-mail address: sclee@mail.kaist.ac.kr (S. Lee).

2. A programmable quantum computer

As shown in [5], a programmable gate array G_B performs an operator $U_B(\theta) = \exp[-i(\theta/2)B]$ of a self-inverse generator B in the following way. The one-qubit program state $|\theta\rangle$ is prepared as

$$|\theta\rangle = \cos(\theta/2)|0\rangle - i \sin(\theta/2)|1\rangle. \quad (1)$$

The data state $|d\rangle$ has an arbitrary dimension 2^n (of n qubits), and $U_B(\theta)$ and B are represented by $2^n \times 2^n$ matrices. The whole state is given by the direct product of the program and data states, $|\theta\rangle \otimes |d\rangle$. Then, G_B consists of sequential applications of a controlled- B and a one-qubit Hadamard operator on the program state. The controlled- B is defined by

$$|0\rangle\langle 0| \otimes E + |1\rangle\langle 1| \otimes B,$$

where E is a unity operator, and E and B are applied on the data state according to the program state. Since $B^2 = E$ and thus $U_B(\theta) = \cos(\theta/2)E - i \sin(\theta/2)B$, the application of G_B gives

$$\begin{aligned} G_B|\theta\rangle|d\rangle &= H[\cos(\theta/2)|0\rangle|d\rangle - i \sin(\theta/2)|1\rangle B|d\rangle] \\ &= \frac{1}{\sqrt{2}}[|0\rangle U_B(\theta)|d\rangle + |1\rangle U_B(-\theta)|d\rangle], \end{aligned} \quad (2)$$

where the symbol ' \otimes ' is omitted for simplicity. A projective measurement of the program state in the basis $\{|0\rangle, |1\rangle\}$ will make the data state collapse into either a desired state $U_B(\theta)|d\rangle$ or wrong state $U_B(-\theta)|d\rangle$ with equal probability. In case of failure, the wrong state can be corrected, with a success probability of 1/2, by another application of G_B using the program state $|2\theta\rangle$. Even if this correction fails again, it is still possible to correct the new wrong state in the same manner as the program state $|2^2\theta\rangle$. The corrections can be repeated until success, and the average number of corrections is only two [3–5]. Therefore, the operator $U_B(\theta)$ is implemented in both programmable and probabilistic ways by G_B .

By extending G_B , a probabilistic universal gate array can be constructed. As is well known, arbitrary operators are implemented by sequences of elementary operators [1]. Since the elementary operators are not unique, preferred elementary operators can be chosen. As our preferred operators for the universal gate array using G_B , NOT gates (σ_x), one-qubit z -rotation operators $R_{\mu z}(\theta) = \exp[-i\theta I_{\mu z}]$, and two-qubit coupling operators $J_{\mu\nu}(\theta) = \exp[-i\theta 2I_{\mu z}I_{\nu z}]$ were selected, where the subscripts μ and ν denote the qubits ($\mu, \nu = A, B, \dots$), and $I_{\mu z}$ is a z -component angular momentum operator. These operators are implemented in the manner of the above scheme and the corresponding circuit is illustrated in Fig. 1 for a two-qubit data state. The information about which operator among NOT, $R_{\mu z}(\theta)$, and $J_{\mu\nu}(\theta)$ will be performed is carried by the command state $|c\rangle$, and θ is stored in the program state [5]. By sequentially supplying $|\theta\rangle$ and $|c\rangle$ corresponding to each elementary oper-

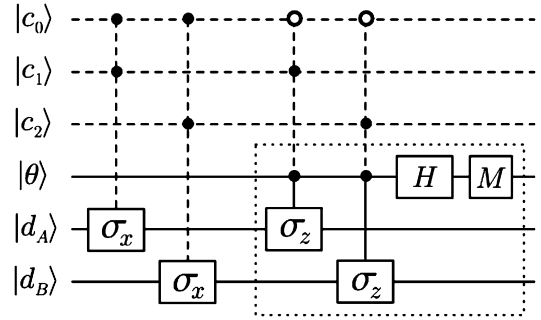


Fig. 1. A universal gate array for a two-qubit data state $|d\rangle = |d_A\rangle \otimes |d_B\rangle$. σ_x and σ_z are Pauli matrices. H is a Hadamard operator and M represents a projective measurement in the basis of $\{|0\rangle, |1\rangle\}$. The dashed lines, command state $|c\rangle = |c_0\rangle \otimes |c_1\rangle \otimes |c_2\rangle$ and related parts, can be realized by the classical computer, and the circuit inside the dotted box was actually realized to implement $J_{12}(\theta)$.

ators, an arbitrary operation can be performed. Note that classical bits are sufficient for the command state, and therefore the command state and the related parts (dashed lines in the figure) can be realized by the classical computer.

3. NMR implementations

We have implemented the above circuit for the case of a one-qubit program state and a two-qubit data state by NMR. Since the classical parts of the circuit can be implicitly realized by the classical computer that controls the NMR instrument, the crucial point is to implement the circuit inside the dotted box in Fig. 1. In the case of a two-qubit data state $|d\rangle = |d_A d_B\rangle = |d_A\rangle \otimes |d_B\rangle$, this circuit can perform $R_{\mu z}(\theta)$ and $J_{AB}(\theta)$ depending on the command state. We have chosen $J_{AB}(\theta)$ for the demonstration, which is a non-separable two-qubit operation unless $\theta = n\pi$ for an integer n , while $R_{\mu z}(\theta)$ is just a one-qubit operation. The initial data state was prepared as $|d\rangle = (|00\rangle + |01\rangle + |10\rangle + |11\rangle)/2$ to show a non-trivial demonstration of $J_{AB}(\theta)$, and θ was chosen to be $\pi/2$ to easily verify whether the execution was successful. The successful projective measurement, after which the program state is collapsed into $|0\rangle$, will make the data state

$$\begin{aligned} J_{AB}(\pi/2)(|00\rangle + |01\rangle + |10\rangle + |11\rangle)/2 \\ = (|00\rangle + i|01\rangle + i|10\rangle + |11\rangle)/2, \end{aligned} \quad (3)$$

neglecting an overall phase.

The projective measurement M is not available in NMR experiments, but can be simulated as follows. Suppose that the data state is, for example,

$$|d\rangle = (|00\rangle + |11\rangle)/\sqrt{2}.$$

A projective measurement on the qubit A in the basis $\{|0\rangle, |1\rangle\}$ will make the state collapse into $|00\rangle$ or $|11\rangle$ with equal probability 1/2. Another measurement on the

qubit B gives $|0\rangle_B$ if the first one gives $|0\rangle_A$, and $|1\rangle_B$ if $|1\rangle_A$. The two measurement results are correlated.

In NMR experiments, such projective measurements are not possible, and measured values are expectation values or ensemble averages. Assume that the expectation value $\langle\sigma_z\rangle$ is given by $\langle 0|\sigma_z|0\rangle = 1$ and $\langle 1|\sigma_z|1\rangle = -1$. It is then obvious that $\langle\sigma_z\rangle_A = \langle\sigma_z\rangle_B = 0$ for the above state, and two values have no correlation that naturally arises in projective measurements.

However, the correlation between two qubits can be obtained from their expectation values with the help of a *correlation operator* [7], which is simply a CNOT gate in this case. From the anti-commutation relation $\{\sigma_i, \sigma_j\} = 2\delta_{ij}$, it holds that $\sigma_x\sigma_z\sigma_x = -\sigma_z$ and thus $\langle\sigma_z\rangle + \langle\sigma_x\sigma_z\sigma_x\rangle = 0$ for any one-qubit state. That is,

$$\langle\psi|\sigma_z|\psi\rangle + (\langle\psi|\sigma_x)\sigma_z(\sigma_x|\psi\rangle) = 0, \quad (4)$$

which means that the expectation values of two experiments with and without applying a NOT gate will cancel each other. Utilizing this fact, the averaged $\langle\sigma_z\rangle_B$ over two experiments with and without a CNOT gate, of which the control bit is the qubit A and the target, the qubit B , will be the very expectation value of the qubit B only when the qubit A is in the state $|0\rangle$. In other words, the expectation value $\langle\sigma_z\rangle_B$ is *filtered* according to the state of the qubit A [7].

Therefore, this corresponds to the simulation of the projective measurement of the case when the qubit A is collapsed into $|0\rangle$. If one wants to simulate the other case, the CNOT (or $|0\rangle\langle 0|_A \otimes E_B + |1\rangle\langle 1|_A \otimes \text{NOT}_B$) is replaced by $|0\rangle\langle 0|_A \otimes \text{NOT}_B + |1\rangle\langle 1|_A \otimes E_B$. In our experiments, the goal of the projective measurement is to collapse the program state into $|0\rangle$, and the available expectation values in NMR are $\langle\sigma_x\rangle$ and $\langle\sigma_y\rangle$. Thus, we have used a controlled- σ_z for the correlation operator since $\sigma_z\sigma_{x(y)}\sigma_z = -\sigma_{x(y)}$.

This filtering can be used for many-qubit cases as originally employed in [7]. However, we note that it is effective when the given state is a *comb state*, a superposition of eigenstates of which non-zero coefficients are equal up to phases. If this condition is not met, the magnitude of filtered expectation values should be considered to determine the states of qubits. In our experiment, the state before the measurement is always a comb state in the basis of the program state, as shown in Eq. (2), and thus the filtering was useful. Also, note that the filtering is only a simulation of the projective measurements in the sense that it gives just the same expectation values, and successive executions of G_B with different program states are not possible.

4. Experiments and results

As qubits, three ^{13}C nuclear spins of 99% carbon-13 labeled alanine in D_2O solvent were used. The experi-

ments were conducted on a Bruker DRX300 spectrometer of 7.4 T magnetic field with proton decoupling. The Hamiltonian of the system reads

$$\mathcal{H} = \sum_i^3 \omega_i I_{iz} + \sum_{i<j}^3 \pi J_{ij} 2I_{iz} I_{jz},$$

where the subscripts i and j denote the spins ($i, j = 1, 2, 3$), ω_i is a Larmor frequency, and J_{ij} is the coupling constant between spins i and j . The Larmor frequencies were measured to be $\omega_1/2\pi \approx 5978$ Hz, $\omega_2/2\pi \approx -3477$ Hz, and $\omega_3/2\pi \approx -6070$ Hz in a rotating frame of $\omega/2\pi = 75.475031$ MHz. The coupling constants J_{12} , J_{23} , and J_{13} were about 54.06, 34.86, and -1.30 Hz, respectively.

From this Hamiltonian and the interaction terms of rf pulses, the rotation operators $R_{i\alpha}(\theta) = \exp[-i\theta I_{i\alpha}]$ (α is x , y or z) and coupling operators $J_{ij}(\theta)$ can be implemented. The system was handled in a triply rotating frame where $\omega_i = 0$, and the reference phase of each qubit was traced during the experiments. $R_{ix(y)}(\theta)$ was realized by spin-selective UBURP or REBURP pulses [8] of about 2 ms in length, $R_{iz}(\theta)$ by adjusting the reference phases of the rotating frame, and $J_{ij}(\theta)$ by time evolution and the appropriate refocusing scheme [9–11].

To obtain results, we performed $3 \times 2 = 6$ experiments: three for an effective pure state [12,13] and two for a simulation of projective measurements. The effective pure state was obtained by three different initial sequences [14]. One is “no operation” that leaves the deviation density matrix in the thermal equilibrium state $\rho_1 = I_{1z} + I_{2z} + I_{3z}$, and the other two sequences are

$$R_{2z}(\pi/2)J'_{23}(\pi/2)R_{2y}(\pi/2)R_{1x}(\pi/2)J'_{12}(\pi/2)R_{1y}(-\pi/2)$$

and

$$R_{1x}(-\pi/2)J'_{12}(\pi/2)R_{1y}(\pi/2)R_{2y}(-\pi/2)J'_{12}(\pi/2) \\ \times J'_{23}(\pi/2)R_{2y}(\pi/2),$$

read from right to left. These sequences transform ρ_1 into $\rho_2 = 4I_{1z}I_{2z}I_{3z} + 2I_{2z}I_{3z} - I_{3z}$ and $\rho_3 = 2I_{1z}I_{2z} + 2I_{1z}I_{3z} + I_{3z}$. The effective pure state is obtained from $\rho_1 + \rho_2 + \rho_3$. $J'_{ij}(\theta)$ denotes $J_{ij}(\theta)R_{kx}(\pi)$ and is easier to implement than $J_{ij}(\theta)$ in our refocusing scheme.

The controlled- σ_z in the circuit is implemented by the sequence

$$J_{ij}(\pi/2)I_{iz}(-\pi/2)I_{jz}(-\pi/2),$$

for the control spin i and the target j . The sequence for H_i , Hadamard operator on spin i , is $R_{iz}(\pi)R_{iy}(-\pi/2)$, and the program state in Eq. (1) is prepared by the sequence $H_i R_{iz}(\theta) H_i$. With these sequences, the experiment took about 95 ms in the longest case. There was no signal averaging in each experiment.

We assigned spins 1 and 3 as the data qubits A and B , and spin 2 as the program qubit, respectively. Fig. 2A shows the reference spectrum of spin 1. The large splitting is due to J_{12} and the small one, J_{13} . Considering

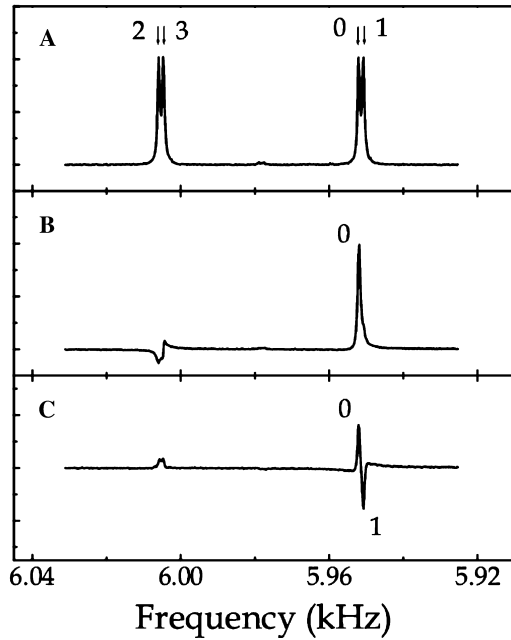


Fig. 2. The result spectra of spin 1 assigned as the data qubit *A*. All the spectra are drawn in the same scale, and the horizontal lines are at zero level of the vertical axes. The spectrum shows (A) the reference, (B) the effective pure state $|000\rangle$ after a read-out pulse, and (C) the final result. See text.

the signs of the coupling constants, the peaks are labeled as peaks 0, 1, 2, and 3, which are observed when spins 2 and 3 are in the states $|00\rangle_{23} = |0\rangle_2 \otimes |0\rangle_3$, $|01\rangle_{23}$, $|10\rangle_{23}$, and $|11\rangle_{23}$, respectively. Each peak is positive when spin 1 is $|x+\rangle = (|0\rangle + |1\rangle)/\sqrt{2}$, and negative when $|x-\rangle = (|0\rangle - |1\rangle)/\sqrt{2}$ because the measured values are $\langle\sigma_x\rangle$. The spectrum of the effective pure state $|000\rangle$ was obtained by a read-out pulse on spin 1, $R_{1y}(\pi/2)$, by which the state becomes $|x+\rangle_1 \otimes |00\rangle_{23}$ and thus the positive peak 0 appears, as shown in Fig. 2B. It is enough to examine only the spectrum of spin 1 to determine the result of the experiment. Since Eq. (3) is rewritten as

$$[(|0\rangle_A + i|1\rangle_A) \otimes |0\rangle_B + (i|0\rangle_A + |1\rangle_A) \otimes |1\rangle_B]/2,$$

and the program state is $|0\rangle$, the first term exhibits a positive peak 0 and the second term a negative peak 1 after adjusting the overall phase of the spectrum, as clearly shown in Fig. 2C. Therefore, the execution of the programmable quantum computer is successfully demonstrated.

It is considered that the main reason for experimental errors is that the spin–spin couplings are not perfectly suppressed during the applications of the pulses. A simple rectangular pulse on a spin *i* along *x* axis results in the rotation of spin *i* about a tilted axis between I_{ix} and I_{iz} axes in the Cartesian subspace spanned by $\{I_{ix}, I_{iy}, I_{iz}\}$ if the pulse is off-resonance [15]. Some shaped pulses such as BURP [8] employed here are designed to suppress this off-resonance effect by

adjusting the strengths of successive rectangular pulses so that the net effect of rectangular pulses is rotation about I_x axis. Even though the pulse is on-resonance, there would exist a spin–spin coupling term between spins *i* and *j*, and the effect of the pulse is rotation about a tilted axis between I_{ix} and $2I_{iz}I_{jz}$ axes in the subspace spanned by $\{I_{ix}, 2I_{iy}I_{jz}, 2I_{iz}I_{jz}\}$. The coupling term $2I_{iz}I_{jz}$ behaves exactly the same as the off-resonance term except that the subspace is different. Therefore, this spin–spin coupling is also suppressed by the shaped pulses. However, not all the couplings are cancel. In our case, the couplings between spins 1 and 2, and 1 and 3 during the application of a shaped pulse on spin 1 are suppressed. But we cannot cancel the coupling between spins 2 and 3, and this is the main cause of the errors shown in Figs. 2B and C. Thus, an adequate method is required to resolve this problem [16,17].

5. Conclusion

We have experimentally demonstrated the feasibility of a programmable quantum computer by NMR. By preparing the program state, different operators can be applied on the data state by the fixed circuit. A non-separable two-qubit operation $J_{AB}(\pi/2)$ was demonstrated in a programmable way. The projective measurement required in the scheme was successfully simulated.

Acknowledgments

This work was supported by the NRL program and KOSEF via eSSC at POSTECH.

References

- [1] A. Barenco et al., Phys. Rev. A 52 (1995) 3457.
- [2] M.A. Nielsen, I.L. Chuang, Phys. Rev. Lett. 79 (1997) 321.
- [3] J. Preskill, Proc. R. Soc. London, Ser A 454 (1998) 385.
- [4] G. Vidal et al., Phys. Rev. Lett. 88 (2002) 047905.
- [5] J. Kim et al., Phys. Rev. A 65 (2002) 012302.
- [6] G. Teklemariam et al., Phys. Rev. A 66 (2002) 012309.
- [7] D. Collins, quant-ph/0111108.
- [8] H. Geen, R. Freeman, J. Magn. Reson. 93 (1991) 93.
- [9] N. Linden et al., Chem. Phys. Lett. 305 (1999) 28.
- [10] J.A. Jones, E. Knill, J. Magn. Reson. 141 (1999) 322.
- [11] D.W. Leung et al., Phys. Rev. A 61 (2000) 042310.
- [12] N. Gershenfeld, I.L. Chuang, Science 275 (1997) 350.
- [13] D.G. Cory et al., Proc. Natl. Acad. Sci. USA 94 (1997) 1634.
- [14] X. Peng et al., quant-ph/0108068.
- [15] R.R. Ernst, G. Bodenhausen, A. Wokaun, Principles of Nuclear Magnetic Resonance in One and Two Dimensions, Oxford University Press, Oxford, 1987.
- [16] L.M.K. Vandersypen et al., Nature (London) 414 (2001) 883.
- [17] E.M. Fortunato et al., J. Chem. Phys. 116 (2002) 7599.